

# Dressing the Imagination: A Dataset for AI-Powered Translation of Text into Fashion Outfits and A Novel KAN Adapter for Enhanced Feature Adaptation

Gayatri Deshmukh  
Independent Researcher  
dgayatri9850@gmail.com

Somsubhra De  
IIT Madras  
22f3002680@ds.study.iitm.ac.in

Chirag Sehgal  
Delhi Technological University  
chiragsehgal224@gmail.com

Jishu Sen Gupta  
IIT BHU  
jishusen.gupta.mat22@itbhu.ac.in

Sparsh Mittal  
IIT Roorkee  
sparsh.mittal@ece.iitr.ac.in

## Abstract

Specialized datasets that capture the fashion industry’s rich language and styling elements can boost progress in AI-driven fashion design. We present **FLORA** (*Fashion Language Outfit Representation for Apparel Generation*), the first comprehensive dataset containing 4,330 curated pairs of fashion outfits and corresponding textual descriptions. Each description utilizes industry-specific terminology and jargon commonly used by professional fashion designers, providing precise and detailed insights into the outfits. Hence, the dataset captures the delicate features and subtle stylistic elements necessary to create high-fidelity fashion designs. We demonstrate that fine-tuning generative models on the FLORA dataset significantly enhances their capability to generate accurate and stylistically rich images from textual descriptions of fashion sketches. FLORA will catalyze the creation of advanced AI models capable of comprehending and producing subtle, stylistically rich fashion designs. It will also help fashion designers and end-users to bring their ideas to life. As a second orthogonal contribution, we introduce KAN Adapters, which leverage Kolmogorov-Arnold Networks (KAN) as adaptive modules. They serve as replacements for traditional MLP-based LoRA adapters. With learnable spline-based activations, KAN Adapters excel in modeling complex, non-linear relationships, achieving superior fidelity, faster convergence and semantic alignment. Extensive experiments and ablation studies on our proposed FLORA dataset validate the superiority of KAN Adapters over LoRA adapters. To foster further research and collaboration, we will open-source

both the FLORA and our implementation code.

## 1. Introduction

Artificial intelligence has become increasingly influential in various industries, fashion being a prominent example. The global fashion industry, valued at approximately 2.4 trillion and growing at an annual rate of 5.5% over the past decade [5], represents a significant economic sector facing constant pressure to innovate and respond to consumer demands. The integration of AI in fashion has revolutionized design processes and enhanced creativity and consumer personalization. AI’s role in fashion extends beyond virtual try-on systems to various applications, including trend forecasting, product development, supply chain optimization, and sustainable practices [30]. For instance, AI algorithms analyze vast datasets from social media and fashion shows to predict upcoming trends, enabling brands to remain competitive. Additionally, AI-powered recommendation systems provide personalized styling suggestions, enhancing the overall shopping experience for consumers.

Despite the potential, AI applications in fashion face several challenges [33]. One major issue is the complexity of fashion design, which involves subjective details like color, style, fabric, and texture. AI models often struggle to capture the nuanced details of fashion sketches. Existing models often produce outputs that lack coherence or fail to align with the provided descriptions [9, 14, 26]. Another challenge is the unavailability of well-annotated datasets, especially sketch-based datasets. Traditional fashion design practices, including seasonal collections and lengthy pro-

duction cycles, often lag behind the fast-paced demands of consumers. As trends evolve rapidly, designers face the challenge of producing timely collections that resonate with audiences. This underscores the need for innovations that streamline design processes to maintain competitiveness.

This research addresses the problem of generating high-fidelity fashion outfit sketches based on detailed text descriptions. Unlike virtual try-on systems [11], which simulate how garments fit on a user, our goal is to create accurate and visually appealing fashion sketches from textual information. Our paper addresses the critical issue of dataset quality by providing a meticulously curated and annotated dataset. Developing a robust pipeline for sketch generation from text can help overcome obstacles in translating descriptive text into coherent and stylistically appropriate visual representations. With this, we aim to advance the capability of AI in fashion design to streamline the design workflow, reducing the time spent on initial sketches, enhancing collaboration, and boosting sales. This will help emerging designers who may not have traditional sketching skills and can serve as a valuable tool for designers, researchers, and other stakeholders in this industry.

Additionally, in today’s landscape, datasets are increasingly complex, with higher levels of non-linearity that make it challenging for models to effectively capture intricate patterns. Models often struggle to adapt to these complexities. For instance, datasets like FLORA present unique challenges due to their emphasis on fine-grained details—such as fabric type, fit, and decorative elements—which require nuanced understanding and multi-modal alignment. These subtle attributes introduce high variability and complexity, making it difficult for models to generalize well from limited data. To address this, we propose the KAN Adapter, which excels at learning non-linearities through its learnable activations, thereby enhancing the model’s ability to capture complex, fine-grained relationships. This paper makes the following key contributions:

- **FLORA Dataset:** We introduce FLORA, a large-scale, curated dataset comprising 4,330 pairs of fashion outfit sketches and detailed textual descriptions. Each description uses industry-specific terminology, capturing the nuanced design elements essential for high-fidelity fashion sketch generation from text. FLORA fills a critical gap in existing resources by providing the first dataset tailored specifically to text-to-fashion sketch generation. FLORA will enable AI models to generate precise, high-quality fashion sketches from textual descriptions, reducing reliance on traditional sketching skills and accelerating the initial design phases.
- **KAN Adapters:** We propose KAN adapters, a new approach that replaces traditional MLP-based LoRA adapters with Kolmogorov-Arnold Networks (KANs) [22]. By enabling complex, non-linear transformation

modeling, KAN Adapters achieve training efficiency and adaptability, making them particularly effective for tasks requiring intricate representation.

- Our experiments show that KAN adapters achieve faster convergence and higher fidelity than LoRA, enabling models to reach optimal performance in fewer training steps. Additionally, fine-tuning generative models on the FLORA dataset greatly improves their ability to produce accurate, stylistically rich images from fashion outfit descriptions.

## 2. Related Works

**Related work on AI in fashion:** Text-to-image generation has rapidly evolved, driven by growing demands for visual content across diverse sectors, including art, marketing, education, and, more recently, fashion [14]. The fashion industry, in particular, has embraced AI to transform design and retail, with major brands like H&M, Zara, and Nike leveraging AI to enhance creativity and efficiency [1, 12]. AI tools now support designers in generating patterns and styles by analyzing consumer preferences, allowing for faster, trend-responsive design cycles. Predictive analytics further empower brands to anticipate fashion trends, enabling the creation of innovative collections that resonate with consumers while facilitating personalized shopping experiences through tailored outfit recommendations.

Generative models like Variational Autoencoders (VAEs) and Generative Adversarial Networks (GANs) have become foundational in creating high-quality garment visuals. These models assist designers by visualizing new styles and enabling quick design iterations. Style transfer models, such as Pix2Pix [13], use conditional GANs [23] for image translation tasks, while FashionGAN [38] allows designers to create virtual model visualizations of new apparel designs. Recently, diffusion models have surpassed GANs in the image generation space [15]. Models like Stable Diffusion [4], OpenAI’s DALL-E 2 [29], and Midjourney have become popular tools in both commercial and non-commercial settings. Such tools have brought AI-driven design automation into practical use, with platforms like DeepAI [2] and RunwayML [3] facilitating novel design and routine automation tasks in fashion media production. Text-to-image models now enable AI to create garment visuals from descriptions using sophisticated transformer architectures, as seen in DALL-E [29], Imagen [32], and Stable Diffusion [8, 31].

However, challenges persist in generating high-fidelity and stylistically accurate images from complex fashion descriptions, particularly for stylized sketches, which are integral to fashion design. While these models excel at realistic image generation, they lack optimization for fashion sketches. Additionally, there are no dedicated datasets that are sufficiently curated and explicitly annotated for the pur-

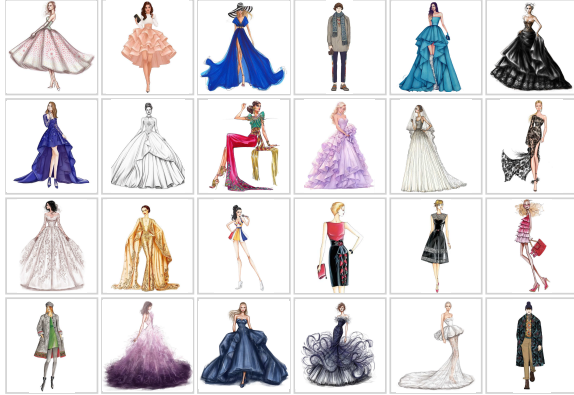


Figure 1. Sample images from our dataset



Figure 2. A figure and the generated textual description pair

pose of generating fashion sketches from text descriptions. This limits the development of robust models for fashion sketch generation.

Current research has made strides in fashion synthesis, including human parsing, pose estimation, landmark detection, style transfer, and clothing simulation. Datasets like Market-1501 [39], DeepFashion [21], and VITON [10] support these applications. However, the specific domain of text-based fashion sketch generation remains unexplored, highlighting a gap for dedicated datasets. We address this gap by proposing a novel dataset tailored for generating fashion sketches from textual descriptions. By focusing on this use case, we aim to lay the groundwork for more specialized and nuanced AI applications in fashion design, providing researchers and designers with valuable resources to drive innovation and creative expression in the industry.

**Related work on KANs:** Kolmogorov-Arnold Networks (KANs) [22], inspired by the Kolmogorov-Arnold representation theorem, offer an interpretable and flexible alternative to traditional MLPs. With learnable edge activations, KANs adaptively learn input relationships, making them effective for complex function approximation and interpretability in data patterns. Fast KAN [18] introduced an adaptation where B-splines are replaced by Radial Basis Functions (RBFs), aiming to reduce the computational overhead associated with splines. ReLU-KAN [28] addresses the computational complexity in traditional KANs by using ReLU and point-wise multiplication, combining KANs’ ”catastrophic forgetting avoidance” with ReLU’s efficiency, making it suitable for inference and training in deep learning frameworks. ConvKANs [6] integrate KAN nonlinear activations into convolutional layers, making them valuable for interpretable applications in computer vision. Li et al., 2024 [18] investigated and redesigned the established U-Net pipeline by integrating KAN layers into the intermediate tokenized representations, resulting in the U-KAN architecture for more efficient medical image segmentation. Yang et al. [37] introduced the Kolmogorov-Arnold Transformer

(KAT) by incorporating KANs into MLP-based transformers and demonstrated that the proposed KAT outperformed all ViT models on traditional vision tasks.

### 3. Proposed FLORA Dataset

We introduce FLORA, a large-scale dataset comprising 4,330 outfit sketch and textual description pairs. Fig. 1 shows some sample images from the dataset. This dataset aims to facilitate the training of generative models for fashion image synthesis, designed specifically for generating fashion sketches based on descriptive inputs. It represents the first dataset of its kind, addressing the significant gap in resources available for sketch-based fashion design.

#### 3.1. Collection of dataset

To create a diverse range of fashion-related sketches, we initiated the process by web-scraping images using various search queries such as ‘fashion-outfit sketches’, ‘fashion illustrations’, ‘wedding-gown sketches’ and ‘fashion pencil sketches’. We, thus, collected 10,042 images. Since these images had various forms of noise, e.g., signatures, watermarks and text overlays, we employed a multi-stage filtering approach (Figure 3) to obtain a suitable dataset.

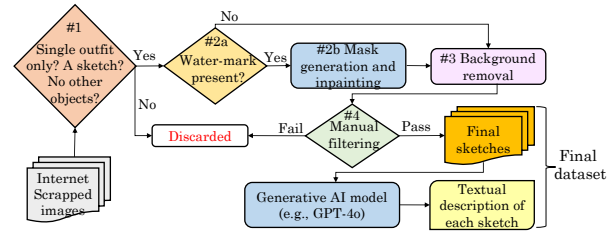


Figure 3. Image filtering steps for creating the training dataset

#### 3.1.1. Multi-Stage Filtering of Images

**1. Prompt-Based Filtering** We first implemented prompt-based filtering using LLaVa 32b [19], a VLLM model. This step checks whether the image is a sketch with only a single outfit and no other objects.

**2. Watermark Removal** Removing signatures and text is crucial for maintaining the visual integrity of the images and improving the model’s ability to learn and generalize effectively. For images with watermark, we applied Keras-OCR [24] for text detection and mask generation followed by ‘ControlNet Stable Diffusion Scene-Text Eraser’ [35] for inpainting. This pipeline effectively removed extraneous elements without distorting the outfits.

**3. Background Removal** We eliminated extraneous objects and color variations for images with distracting background noise. Specifically, we replaced the original backgrounds with clean, transparent ones using a background-remover model [34]. This enhances their visual clarity and ensures the focus remains on the main subject.

**4. Manual Filtering** Finally, we manually checked each image to remove duplicates. We split the images containing multiple sketches into separate sketches to maximize the number of usable samples. We concluded with 4,330 clean and relevant images.

### 3.1.2. Generating description of each sketch

We utilized a multimodal model, viz., OpenAI’s GPT-4o [25] to generate the image descriptions. Each outfit description is structured to include the *human model pose* that consists of the model’s posture, including the position of hands and legs, allowing for accurate sketch recreation, *outfit details*, its *color* and *accessories* that lists any additional elements like shoes or jewelry. Fig. 2 shows an example of one such outfit description. Further details on the dataset and the prompts used are available in the supplementary section.

## 3.2. Dataset Applications & Uniqueness

Our dataset fills a critical gap in fashion image generation and description-based design, particularly in outfit generation, where existing datasets are scarce. It benefits designers by reducing the manual effort required for sketching and gives them a solid foundation to develop their skills and ideas. It empowers non-designers to express creative ideas through text-to-sketch platforms. While existing datasets focus on virtual try-on or human pose estimation [36], our emphasis on sketches adds novelty, making it a valuable tool for advancing creativity and innovation in AI-driven fashion design.

## 4. Proposed KAN Adapter

As a second orthogonal contribution, we propose KAN adapters. In this Section, we first provide a background on LoRA and KAN modules (Sections 4.1-4.2), and then discuss our proposed KAN adapter (Section 4.3).

### 4.1. Background on LoRA modules

LoRA (Low-Rank Adaptation) modules provide an efficient way to fine-tune large models by optimizing the number of

trainable parameters. Instead of adjusting all parameters, which can lead to “catastrophic forgetting”, LoRA adds trainable adapters that preserve the model’s learned features while achieving similar or improved results. These adapters work by training a new set of weights in a reduced dimension (or rank) that are scaled down based on model size. During fine-tuning, the model’s original layers are frozen. LoRA’s linear adapters process the input in parallel, scaling it down to a lower rank and then back to the output dimension. This setup prevents increased inference latency and makes it suitable for various downstream tasks. A formal representation of the LoRA is given in the equation

$$L'(x) = L(x) + W_{\text{up}}(\text{GeLU}(W_{\text{down}}(x))) \quad (1)$$

where  $W_{\text{up}} \in \mathbb{R}^{(d,l)}$  and  $W_{\text{down}} \in \mathbb{R}^{(l,d)}$ , with  $l < d$ . Here,  $W_{\text{up}}$  and  $W_{\text{down}}$  represent the LoRA weights,  $L'(x)$  represents the modified layer output, and  $L(x)$  represents the original layer output to which LoRA is applied. The matrix  $W_{\text{down}}$  is initialized with the distribution of the weights of  $L(x)$  to maintain coherence with the frozen layer.

### 4.2. Background on KANs

Kolmogorov-Arnold Networks (KANs) [22] have been recently introduced as an alternative to traditional MLPs in deep learning applications. Unlike MLPs, which use fixed activation functions, KANs employ learnable B-spline functions as activation layers, making them more flexible and expressive while requiring fewer parameters. B-splines, composed of polynomial segments with control points, allow local adjustments in the activation function without impacting the rest of the network. This local control helps maintain smoothness and facilitates differentiability, which is crucial for efficient backpropagation.

KANs are based on the Kolmogorov-Arnold representation theorem (KART), which states that any continuous high-dimensional function can be decomposed into a sum of univariate functions. Liu et al. [22] extended this to deep networks by creating the KAN-Layer, which consists of learnable activation functions given by the equation:

$$\varphi(x) = w(b(x) + \text{spline}(x)) \quad (2)$$

where,  $b(x) = \text{silu}(x) = x/(1 + e^{-x})$  and  $\text{spline}(x)$  is a linear combination of learnable B-splines. This structure allows KANs to capture complex functions effectively.

### 4.3. Proposed KAN Adapter

The need for adaptable and computationally efficient models has grown recently, especially in domains where fine-tuning large models for downstream tasks can be computationally expensive. Traditional methods like LoRA modules (Section 4.1) address this need by introducing learnable parameters in a lower-dimensional space, typically employing MLPs for transformation. However, MLPs face limitations in efficiently modeling complex non-linear transformations.

To overcome these limitations, we propose KAN Adapters, a novel approach leveraging Kolmogorov-Arnold Networks (KANs) with learnable spline-based activation functions. This architecture efficiently approximates complex, highly non-linear functions, enhancing parameter efficiency and flexibility. Replacing MLP-based LoRA with a KAN adapter improves computational efficiency and adaptability, making it well-suited for tasks requiring sophisticated non-linear representations.

The KAN adapter architecture, illustrated in Figure 4, incorporates KAN as an adapter layer alongside the pre-trained model’s MLP layer. The KAN adapter layer processes input  $X$ , which includes down-projection ( $\phi_{down}$ ) and up-projection ( $\phi_{up}$ ) functions. These functions transform the input to a lower-dimensional space and then project it back, producing  $X'$  using learnable, spline-based activation functions. The outputs from the MLP and KAN adapters are then aggregated and passed to the subsequent layer. For explanatory purposes, we used the MLP layer to add KAN adapters in parallel; however, similar to LoRA, these adapters can be added to any layer.

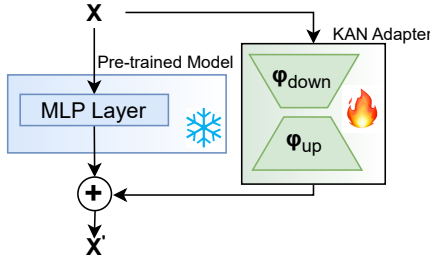


Figure 4. Integration of the KAN Adapter with a pre-trained model. Snowflake symbol (❄) indicates frozen weights, and the fire symbol 🔥 denotes trainable weights.

As depicted in Figure 5, the input  $X \in \{x_1, x_2, x_3, \dots, x_m\}$  is projected into a lower-dimensional representation  $H \in \{h_1, h_2, h_3, \dots, h_n\}$ , where  $X \in \mathbb{R}^m$ ,  $H \in \mathbb{R}^n$ , with  $n = m/2$ , through

$$\phi_{down}(X) = W_b^{down} \cdot g(X) + W_s^{down} \left( \sum_{i=1}^n c_i \gamma(X) \right) \quad (3)$$

Here,  $W_b^{down}$  and  $W_s^{down}$  are learnable stabilizing matrices,  $g(X)$  is an activation function, and  $\gamma_i(X)$  represents a set of basis functions (such as B-splines or Radial Basis Functions). The terms  $c_i$  are the coefficients learned during training. The transformed representation  $H$  is projected back to the original feature space  $\mathbb{R}^m$ .

$$\phi_{up}(X) = W_b^{up} \cdot g(H) + W_s^{up} \left( \sum_{i=1}^m d_i \gamma(H) \right) \quad (4)$$

$W_b^{up}$  and  $W_s^{up}$  are additional stabilization matrices,  $d_i$  are learned coefficients, and  $\gamma_i(H)$  is the basis function representation in the compressed space. This up-projection allows the model to re-expand the representation to the original space while retaining the most relevant features. Finally,

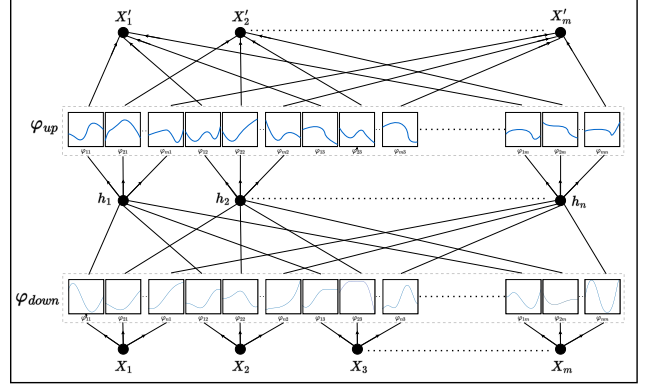


Figure 5. KAN Adapter

outputs from the KAN adapter and MLP are aggregated as

$$X' = \mathcal{L}_\theta(X) + (\phi_{up} \cdot \phi_{down})(X) \quad (5)$$

$\mathcal{L}_\theta(\cdot)$  is the original pre-trained model. The final aggregated output  $X'$  is then passed to subsequent layers, ensuring that the KAN adapter’s non-linear transformations complement the MLP’s capabilities. This complements the main model by introducing non-linear transformations, which LoRA’s MLP layers cannot capture efficiently.

**Salient features:** KAN Adapters differ fundamentally from LoRA’s fixed MLP-based transformations by utilizing flexible, learnable basis functions. This enables KAN Adapters to capture fine-grained patterns within the data, which is crucial for tasks where complex dependencies must be learned. While LoRA adapters are designed to prevent catastrophic forgetting by keeping the core model weights frozen, KAN Adapters offer an additional layer of resilience through their unique use of adaptive, learnable activation functions. Unlike static activations in MLP-based LoRA, the KAN Adapter’s non-linear functions can dynamically adjust to new tasks, selectively retaining important representations from prior tasks without overwriting them. This flexibility enables KAN Adapters to handle the complexities of sequential learning better, as they can modulate responses specifically for new data while preserving critical knowledge from earlier tasks. This added adaptability has been shown in related studies, such as ReLU-KAN [28], to provide enhanced memory retention, making KAN Adapters particularly suited for continual learning scenarios. Additionally, KAN Adapters demonstrate faster convergence compared to LoRA (refer to Figure 6). This faster convergence implies that KAN Adapters can reach optimal or near-optimal performance in fewer training steps, making them more computationally efficient.

## 5. Experimental Section

**Implementation Details:** All models were fine-tuned with a batch size of 12 using gradient accumulation steps of 12, leveraging the AdamW optimizer for enhanced generalization through weight decay. The initial learning rate was set

to  $1 \times 10^{-5}$  and dynamically adjusted with a cosine annealing schedule, gradually varying between a minimum of  $1 \times 10^{-7}$  and a maximum of  $2 \times 10^{-3}$ . This scheduling approach allowed for smooth convergence by reducing the learning rate as training progressed. The training was conducted on a robust setup of 4 x 8 Nvidia H100 GPUs with 80GB VRAM. For all the baselines, elastic weight consolidation [16] was performed to determine where to add LoRA and KAN adapters.

**Test Set:** To evaluate the proposed KAN adapter and demonstrate this dataset’s practical relevance, we created a test set of 500 innovative fashion outfit descriptions. Each description was generated using a structured prompt (refer supplementary) with GPT-4o [25], incorporating standard industry-specific terminology. We introduce novel and unique design elements in the prompts to assess the models’ capability to interpret both familiar and innovative fashion concepts. Thus, our experiments showcase the effectiveness of the dataset in real-world applications.

### 5.1. Quantitative Results

We have conducted text-to-image generation experiments using several baseline models: Stable Diffusion (SD) [31], SD-XL [27], SD 3 [8], Pixart-Sigma [7], and FLUX [17]. In the zero-shot setting, pre-trained baseline models are used to perform inference on our test set without any fine-tuning on FLORA. For KAN adapter, we used radial basis function. We evaluated each model’s performance using FID (Fréchet Inception Distance) for image realism and CLIP-SIM for semantic alignment with textual prompts.

From Table 1, the zero-shot results indicate that while these pre-trained models can produce realistic images to some extent, their semantic alignment with our specific fashion-focused textual prompts remains limited. This performance gap highlights FLORA’s unique characteristics, including fashion-specific terminology and novel design elements that the pre-trained models are not optimized to interpret effectively. From Table 1, KAN adapters consistently outperform LoRA modules across all models, showing superior adaptability and expressive power. KAN’s ability to operate in a lower-dimensional, flexible space enhances its capacity to capture complex data patterns more effectively than LoRA, which relies on MLP layers and is more constrained in its representational flexibility.

Among the models, FLUX with KAN adapters achieved the best overall performance, with an FID of 6.05 and a CLIPSIM of 0.3412. Flux’s advantage stems from its large training dataset and flow-matching algorithm, which aligns the model’s output and data distributions along a linear trajectory in latent space. This approach minimizes sampling steps, improving efficiency and image quality, which KAN adapters further enhance by capturing nuanced details and alignment with prompts.

Methods	Zero-shot		LoRA		KAN	
	FID↓	CLIPSIM↑	FID↓	CLIPSIM↑	FID↓	CLIPSIM↑
FLUX[17]	09.09	0.3112	07.88	0.2987	<b>06.05</b>	<b>0.3412</b>
SD[31]	19.25	0.0623	17.32	0.0910	<b>16.51</b>	<b>0.1112</b>
SD-XL[27]	16.37	0.1539	15.32	0.1522	<b>13.33</b>	<b>0.1897</b>
SD-3[8]	13.28	0.2118	09.37	0.2119	<b>08.07</b>	<b>0.2503</b>
Pixart-Sigma[7]	14.11	0.2666	09.89	0.2542	<b>08.28</b>	<b>0.2991</b>

Table 1. Quantitative evaluation of SOTA diffusion models for generating prompt-based sketches of outfits, using zero-shot, traditional MLP-based LoRA, and our proposed KAN-adapters.

The Stable Diffusion series (SD, SD-XL, SD-3) also saw substantial improvements with KAN adapters, particularly SD-3, which achieved an FID of 8.07 and a CLIP-SIM of 0.2503. KAN’s adaptability allows these models to capture fine-grained visual features that traditional LoRA modules might miss, enhancing both realism and semantic alignment. KAN adapter also improved Pixart-Sigma’s performance, reducing its FID from 9.89 to 8.28 and raising CLIPSIM from 0.2542 to 0.2991. Further, as shown in Figure 6, KAN demonstrates faster convergence and lower loss, indicating improved stability and performance in capturing relevant features.

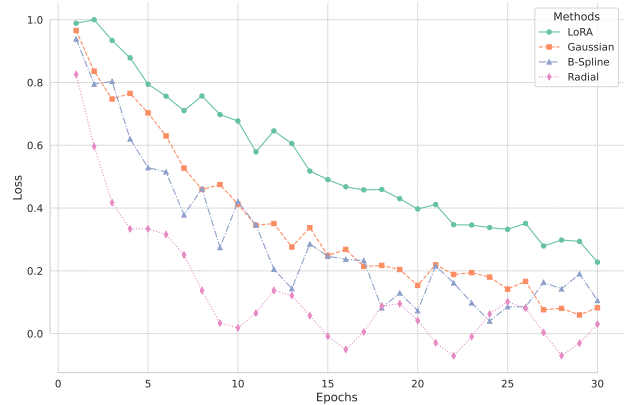


Figure 6. Comparison of LoRA and KAN adapters (using Gaussian, B-Spline, and Radial basis functions) on the FLUX model.

We also conducted a comprehensive human evaluation of each generated sketch, drawing inspiration from EvalCrafter [20]. One sketch was generated for each of the 500 textual descriptions in the test set. A unique set of 500 individuals evaluated each of these 500 sketches. To assess various dimensions of sketch quality, users evaluated them on several key parameters: Prompt Relevance, Visual Quality, Creativity, Pose and Model Accuracy, Color Palette Alignment, Contextual Fit, and Overall Appeal (refer to supplementary for more details). These metrics help quantify their visual observations and provide a structured analysis of each model’s performance. The aggregated results are presented in Table 2. Our findings indicate that FLUX, fine-tuned with the KAN-adapter, outperforms all other models and their respective variants. Additionally, models fine-tuned with the KAN adapter consistently out-

Model	Prompt Relevance		Visual Quality				Creativity			Pose & Model Acc.			Color Palette Alignment		Contextual Fit		Overall Appeal		Latency (s)	
FLUX	59.78	61.43	45.25	46.98	52.29	56.54	65.19	69.78	60.19	63.33	45.92	50.27	46.72	50.33	8.73	8.81				
SD	37.76	39.21	29.92	34.12	19.45	21.21	15.53	18.71	41.18	45.78	18.76	20.21	20.21	22.76	13.43	14.42				
SD-XL	44.78	47.12	33.33	36.54	25.77	29.30	29.92	33.47	48.93	50.21	27.76	31.19	30.33	33.89	9.87	10.02				
SD-3	53.32	56.98	40.14	44.27	37.82	41.65	59.12	63.45	54.44	57.02	39.31	42.75	39.72	44.36	10.11	10.23				
Pixart	51.39	55.03	39.19	41.14	35.71	40.21	61.29	65.43	53.53	56.92	38.27	40.91	36.64	40.19	6.32	6.89				

Table 2. The results represent the percentage of images with a score above 7.5 out of 10, as rated by 500 humans on both LoRA and KAN adapters. The last column shows inference latency. Each reported value is in the format <LoRA>|<KAN-adapter>. For all metrics, except latency, higher is better (acc.= accuracy). Number of diffusion steps: FLUX (20), SD (50), SD-XL and SD-3 (25), Pixart (15).

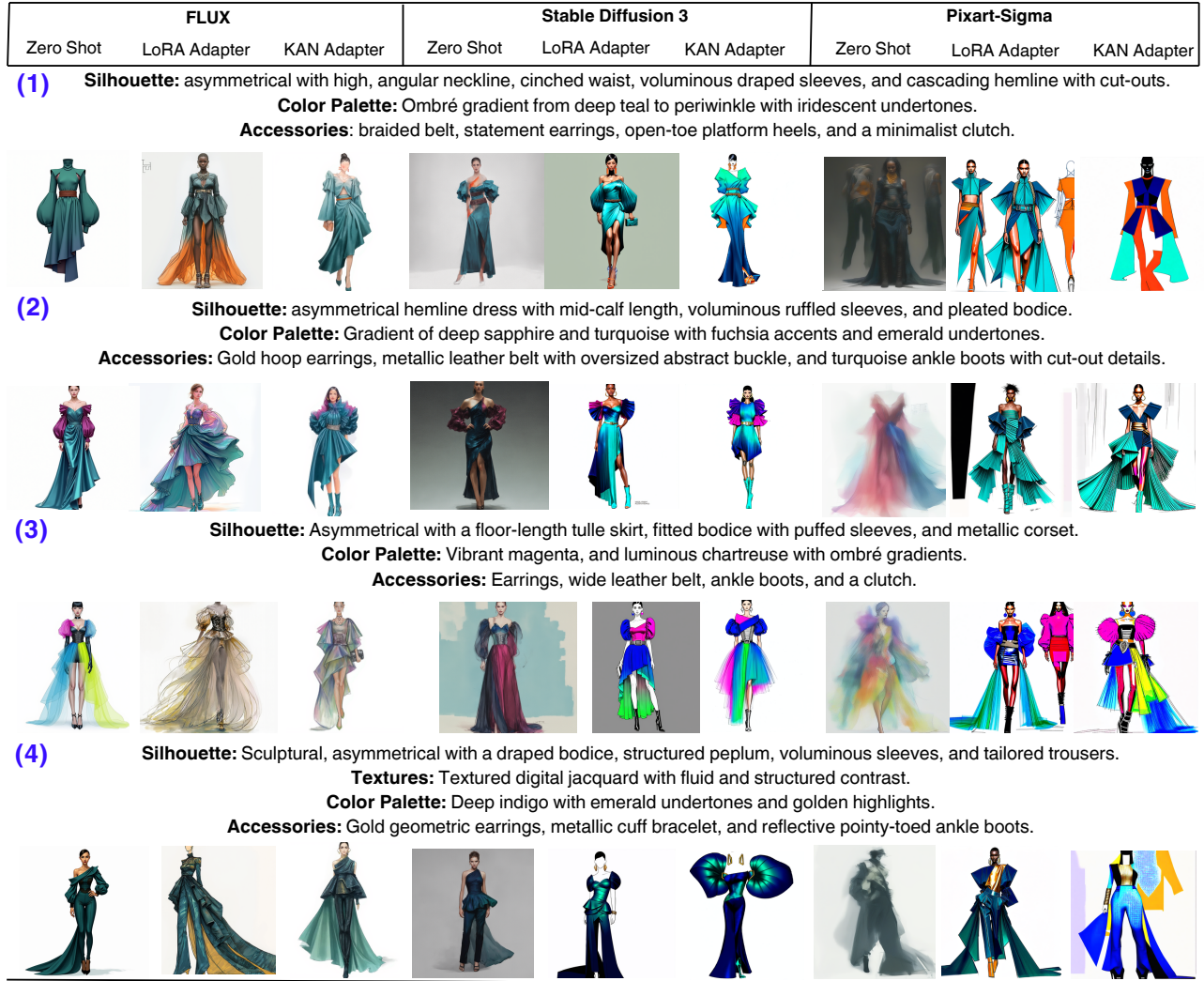


Figure 7. Images generated by various models for zero-shot, LoRA and KAN adapters, given the prompts from the test set. Given the length of original prompts, only condensed versions with key elements are shown here.

perform LoRA across all evaluation parameters. Additionally, Table 2 compares the computational efficiency of each adapter type across various baselines. Each method was evaluated by the number of diffusion steps required to achieve a target performance level. The results indicate

that KAN adapters generally have slightly higher inference times compared to LoRA. However, considering additional factors such as convergence speed during fine-tuning (Figure 6) and KAN’s effectiveness in adapting to non-linear patterns, this modest increase in inference time is a rea-

sonable trade-off for the improved adaptability and performance that KAN offers.

## 5.2. Qualitative Results

To assess the effectiveness of our dataset and the proposed KAN adapter, we conducted qualitative comparisons across FLUX, Pixart-Sigma, and SD3 in Zero-Shot, LoRA, and KAN Adapter settings (refer Figure 7). The evaluation reveals both the need for fine-tuning with a specialized dataset and the performance advantages of KAN over LoRA.

In Zero-Shot settings, the models consistently failed to capture specific fashion-related terminologies and intricate details. For instance, when generating an outfit with an asymmetrical silhouette and angular neckline (Prompt 1), FLUX in Zero-Shot mode overlooked the angular neckline and accessories like the braided belt and clutch. This highlights the model’s inability to interpret nuanced fashion elements without tailored training. However, after fine-tuning with our dataset, FLUX LoRA captured basic elements like the cascading hemline, while FLUX KAN successfully captured all the details, including the braided belt and clutch. This demonstrates the proposed dataset’s importance in teaching models to interpret and represent fashion-specific terms accurately.

As shown in Figure 7, models using the KAN adapter consistently capture more detailed features and produce more aligned sketches, e.g., in Prompt 3, which featured an asymmetrical silhouette with a metallic corset, floor-length skirt, and vibrant color palette, FLUX with LoRA captured the general silhouette but omitted finer details like the metallic corset and specific color variations. FLUX with KAN, in contrast, accurately represented the metallic corset, asymmetrical design, and color specifications, including accessories like earrings and clutch. This highlights KAN’s superiority in understanding nuanced detail, particularly in complex fashion elements.

We extend the qualitative evaluation by presenting t-SNE plots for each baseline and its variants. Figure 8 illustrates optimal feature clustering in model variants fine-tuned with KAN adapters, with different colors representing distinct clusters. This optimal clustering indicates well-learned latent spaces, as tightly grouped clusters suggest that the model has effectively captured nuanced features relevant to each category. Notably, FLUX exhibits the most distinct and cohesive clustering, which aligns with our other observations, further validating the superior generalization and feature representation achieved by this model.

## 6. Ablation Study

To investigate the impact of different basis functions in the KAN adapter, we consider primarily three types of multivariate function-approximating polynomials: B-Spline, standard Radial Basis Function (RBF), and Gaussian. As

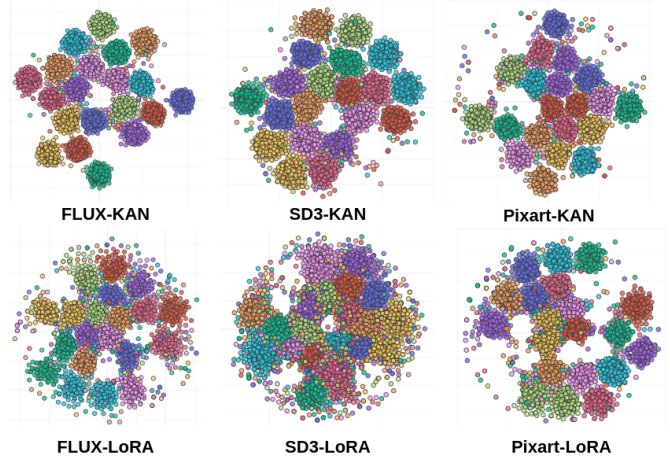


Figure 8. t-SNE plots using KAN and LoRA adapters.

KAN Layers	FID↓	CLIPSIM↑
B-Spline	6.18	0.3002
Radial Basis Function	<b>6.09</b>	0.3276
Gaussian	6.33	<b>0.3301</b>

Table 3. Ablation study results based on KAN Layers

shown in Table 3, the B-Spline basis achieved an FID of 6.18 and a CLIPSIM score of 0.3002, marking it as a middle-ground performer. B-splines, being piecewise polynomials, excel at providing localized control over the function, which is helpful for smooth approximations. However, unlike RBFs, they are sensitive to grid-based recalculations and re-scaling, which can limit their stability and efficiency in higher-dimensional applications.

In contrast, the standard RBF delivered the lowest FID (6.09) and a strong CLIPSIM of 0.3276, achieving the best balance between sample realism and representational consistency. Unlike Gaussian RBFs, which rely on a fixed decay rate, standard RBFs are not bound to a specific decay, allowing them to adapt to complex patterns in data flexibly. This flexibility may explain its superior FID, as it maintains realistic details more effectively than Gaussian and B-Spline functions.

While slightly higher in FID (6.33), the Gaussian basis recorded the highest CLIPSIM at 0.3301, suggesting that it prioritizes structural consistency over fine-grained details. Gaussian functions have smooth and symmetrical decay properties, promoting stability in feature representation but at the cost of adaptability. This fixed decay makes it less effective at capturing localized detail than the general RBF, as seen in the higher FID score. An ablation study examining the impact of KAN downsample rates and LoRA rank is provided in the supplementary section.

## 7. Conclusion

We introduced FLORA, the first dataset crafted specifically for generating fashion outfits from text descriptions, along



with KAN Adapters, architecture leveraging Kolmogorov-Arnold Networks for enhanced model adaptability. Together, these contributions address the lack of high-quality data in AI-driven fashion design and effective modeling techniques. Looking forward, we plan to expand FLORA to train models capable of modifying specific parts of an outfit sketch based on design requirements, allowing designers to easily adjust individual elements while maintaining the overall style. This advancement could enable adaptable AI-powered design tools, fostering a more interactive and flexible approach to fashion creation.

## References

- [1] <https://www.thomasnet.com/insights/zara-h-m-fast-fashion-ai-supply-chain/>. [Online; accessed 07-Oct-2024]. 2
- [2] Deep AI, Inc. <https://deepai.org/>, 2017. [Online; accessed 05-June-2024]. 2
- [3] Inc. Runway AI. <https://runwayml.com/>, 2022. [Online; accessed 05-June-2024]. 2
- [4] Stability AI. Stable diffusion public release. <https://stability.ai/news/stable-diffusion-public-release>, 2022. [Online; accessed 05-July-2024]. 2
- [5] Imran Amed, Achim Berg, Vivek Balchandani, Saskia Hedrich, Robb Rölkens, and Kanaiya Young. The state of fashion 2022, 2022. Accessed: 2024-11-09. 1
- [6] Alexander Dylan Bodner, Antonio Santiago Tepsich, Jack Natan Spolski, and Santiago Pourteau. Convolutional kolmogorov-arnold networks. *arXiv preprint arXiv:2406.13155*, 2024. 3
- [7] Junsong Chen, Chongjian Ge, Enze Xie, Yue Wu, Lewei Yao, Xiaozhe Ren, Zhongdao Wang, Ping Luo, Huchuan Lu, and Zhenguo Li. Pixart-sigma: Weak-to-strong training of diffusion transformer for 4k text-to-image generation, 2024. 6
- [8] Patrick Esser, Sumith Kulal, Andreas Blattmann, Rahim Entezari, Jonas Müller, Harry Saini, Yam Levi, Dominik Lorenz, Axel Sauer, Frederic Boesel, Dustin Podell, Tim Dockhorn, Zion English, Kyle Lacey, Alex Goodwin, Yan-nik Marek, and Robin Rombach. Scaling rectified flow transformers for high-resolution image synthesis, 2024. 2, 6
- [9] Tham Yik Foong, Shashank Kotyan, Po Yuan Mao, and Danilo Vasconcellos Vargas. The challenges of image generation models in generating multi-component images, 2023. 1
- [10] Xintong Han, Zuxuan Wu, Zhe Wu, Ruichi Yu, and Larry S Davis. Viton: An image-based virtual try-on network. In *CVPR*, 2018. 3
- [11] Jianhua Hu, Weimei Wu, Mengjun Ding, Xi Huang, Zhi Jian Deng, and Xuankai Li. A virtual try-on system based on deep learning. In *2023 3rd International Symposium on Computer Technology and Information Science (ISCTIS)*, pages 103–107, 2023. 2
- [12] Fashion AI In 2024: What is Trending This Year. <https://www.intelista.com/fashion-ai-in-2023-what-should-we-expect-to-see-this-year/>. [Online; accessed 07-Oct-2024]. 2
- [13] Phillip Isola, Jun-Yan Zhu, Tinghui Zhou, and Alexei A Efros. Image-to-image translation with conditional adversarial networks. *CVPR*, 2017. 2
- [14] Dora Ivezić and Marina Bagić Babac. Trends and challenges of text-to-image generation: Sustainability perspective. *Croatian Regional Development Journal*, 4:56–77, 2023. 1, 2
- [15] Harry H. Jiang, Lauren Brown, Jessica Cheng, Mehtab Khan, Abhishek Gupta, Deja Workman, Alex Hanna, Johnathan Flowers, and Timnit Gebru. Ai art and its impact on artists. In *Proceedings of the 2023 AAAI/ACM Conference on AI, Ethics, and Society*, page 363–374, New York, NY, USA, 2023. Association for Computing Machinery. 2
- [16] James Kirkpatrick, Razvan Pascanu, Neil Rabinowitz, Joel Veness, Guillaume Desjardins, Andrei A Rusu, Kieran Milan, John Quan, Tiago Ramalho, Agnieszka Grabska-Barwinska, et al. Overcoming catastrophic forgetting in neural networks. *Proceedings of the national academy of sciences*, 114(13):3521–3526, 2017. 6
- [17] Black Forest Labs. black-forest-labs/FLUX.1-dev · Hugging Face. <https://huggingface.co/black-forest-labs/FLUX.1-dev>, 2024. [Online; accessed 05-October-2024]. 6
- [18] Chenxin Li, Xinyu Liu, Wuyang Li, Cheng Wang, Hengyu Liu, and Yixuan Yuan. U-kan makes strong backbone for medical image segmentation and generation. *arXiv preprint arXiv:2406.02918*, 2024. 3
- [19] Haotian Liu, Chunyuan Li, Qingyang Wu, and Yong Jae Lee. Visual instruction tuning. In *NeurIPS*, 2023. 3
- [20] Yaofang Liu, Xiaodong Cun, Xuebo Liu, Xintao Wang, Yong Zhang, Haoxin Chen, Yang Liu, Tiejiong Zeng, Raymond Chan, and Ying Shan. Evalcrafter: Benchmarking and evaluating large video generation models. In *Proceedings of the IEEE/CVF Conference on Computer Vision and Pattern Recognition*, pages 22139–22149, 2024. 6
- [21] Ziwei Liu, Ping Luo, Shi Qiu, Xiaogang Wang, and Xiaoou Tang. DeepFashion: Powering Robust Clothes Recognition and Retrieval with Rich Annotations. In *Proceedings of IEEE Conference on Computer Vision and Pattern Recognition (CVPR)*, 2016. 3
- [22] Ziming Liu, Yixuan Wang, Sachin Vaidya, Fabian Ruehle, James Halverson, Marin Soljačić, Thomas Y. Hou, and Max Tegmark. Kan: Kolmogorov-arnold networks, 2024. 2, 3, 4
- [23] Mehdi Mirza and Simon Osindero. Conditional generative adversarial nets, 2014. 2
- [24] Fausto Morales. Keras-OCR Documentation. <https://keras-ocr.readthedocs.io/en/latest/>, 2019. [Online; accessed 05-July-2024]. 4
- [25] OpenAI. Hello GPT-4o. <https://openai.com/index/hello-gpt-4o/>, 2024. [Online; accessed 20-September-2024]. 4, 6
- [26] Khushboo Patel. Advancements and challenges in text-to-image synthesis: A comprehensive review. *International Journal of Intelligent Systems and Applications in Engineering*, 12(3):4228–4237, 2024. 1

- [27] Dustin Podell, Zion English, Kyle Lacey, Andreas Blattmann, Tim Dockhorn, Jonas Müller, Joe Penna, and Robin Rombach. Sdxl: Improving latent diffusion models for high-resolution image synthesis, 2023. 6
- [28] Qi Qiu, Tao Zhu, Helin Gong, Liming Chen, and Huansheng Ning. Relu-kan: New kolmogorov-arnold networks that only need matrix addition, dot multiplication, and relu. *arXiv preprint arXiv:2406.02075*, 2024. 3, 5
- [29] Aditya Ramesh, Mikhail Pavlov, Gabriel Goh, Scott Gray, Chelsea Voss, Alec Radford, Mark Chen, and Ilya Sutskever. Zero-shot text-to-image generation, 2021. 2
- [30] Bharati Rathore. Artificial intelligence in sustainable fashion marketing: Transforming the supply chain landscape. *Edu-zone : international peer reviewed/refereed academic multi-disciplinary journal*, 8:2319–5045, 2019. 1
- [31] Robin Rombach, Andreas Blattmann, Dominik Lorenz, Patrick Esser, and Björn Ommer. High-resolution image synthesis with latent diffusion models. In *Proceedings of the IEEE/CVF Conference on Computer Vision and Pattern Recognition (CVPR)*, pages 10684–10695, 2022. 2, 6
- [32] Chitwan Saharia, William Chan, Saurabh Saxena, Lala Li, Jay Whang, Emily Denton, Seyed Kamyar Seyed Ghasemipour, Burcu Karagol Ayan, S. Sara Mahdavi, Rapha Gontijo Lopes, Tim Salimans, Jonathan Ho, David J Fleet, and Mohammad Norouzi. Photorealistic text-to-image diffusion models with deep language understanding, 2022. 2
- [33] Mariapaola Saponaro, Diane Le Gal, Manjiao Gao, Matthieu Guisiano, and Ivan Coste Maniere. Challenges and opportunities of artificial intelligence in the fashion world. In *2018 International Conference on Intelligent and Innovative Computing Applications (ICONIC)*, pages 1–5, 2018. 1
- [34] schroneko. Transparent Background - a Hugging Face Space by schroneko. <https://huggingface.co/spaces/schroneko/transparent-background>, 2024. [Online; accessed 05-July-2024]. 4
- [35] Onkar Susladkar. Controlnet Stable diffusion scene text Eraser. [https://huggingface.co/onkarsus13/controlnet\\_stablediffusion\\_scenetextEraser](https://huggingface.co/onkarsus13/controlnet_stablediffusion_scenetextEraser), 2024. [Online; accessed 25-September-2024]. 4
- [36] Kota Yamaguchi, M. Hadi Kiapour, Luis E. Ortiz, and Tamara L. Berg. Parsing clothing in fashion photographs. In *2012 IEEE Conference on Computer Vision and Pattern Recognition*, pages 3570–3577, 2012. 4
- [37] Xingyi Yang and Xinchao Wang. Kolmogorov-arnold transformer. *arXiv preprint arXiv:2409.10594*, 2024. 3
- [38] Cui Yirui, Q. Liu, C. Gao, and Zhuo Su. Fashiongan: Display your fashion design using conditional generative adversarial nets. *Computer Graphics Forum*, 37:109–119, 2018. 2
- [39] Liang Zheng, Liyue Shen, Lu Tian, Shengjin Wang, Jingdong Wang, and Qi Tian. Scalable person re-identification: A benchmark. In *Proceedings of the IEEE International Conference on Computer Vision (ICCV)*, 2015. 3

# Dressing the Imagination: A Dataset for AI-Powered Translation of Text into Fashion Outfits and A Novel KAN Adapter for Enhanced Feature Adaptation

## Supplementary Material

### 8. Fine-Tuning Template for Outfit Sketch Generation

We developed a structured prompt template for fine-tuning the models. This template was designed to capture essential aspects of each outfit sketch, including model presence, gender, pose, outfit description, color details and accessories. By standardizing these attributes, we aimed to provide the model with clear, detailed inputs that could guide the generation process toward accurate, high-quality fashion sketches. The template used is as follows:

```
MODEL PRESENCE: {MODEL_PRESENCE}
MODEL GENDER: {MODEL_GENDER}
MODEL POSE: {MODEL_POSE}
OUTFIT DESCRIPTION: {OUTFIT_DESCRIPTION}
COLOR DETAILS: {COLOR_DETAILS}
ACCESSORIES: {ACCESSORIES}
```

### 9. Detailed Description of Human Evaluation Metrics

For a thorough evaluation of the generated fashion sketches, we defined seven key metrics, each capturing specific aspects of image quality and alignment with the prompt. The main paper presents human evaluation results (refer to Table 2). These metrics allowed us to perform a comprehensive assessment, ensuring that both technical quality and alignment with the prompt are rigorously evaluated:

- **Prompt Relevance:** Evaluates how accurately the generated image reflects the essential elements described in the prompt. This metric focuses on effectively visualizing the main idea or theme specified.
- **Visual Quality:** Assesses the technical quality of the image, including factors such as resolution, sharpness, clarity, and the overall visual appeal.
- **Creativity:** Measures the degree of innovation and imaginative interpretation in the image. This metric considers how the generated image demonstrates creativity while staying coherent with the prompt’s details.
- **Pose and Model Accuracy:** Examines the alignment between the model’s physical representation in the image, such as pose, gender, and stance and the specifications given in the prompt.
- **Color Palette Alignment:** Compares the colors used in the generated image to the colors described in the prompt, assessing accuracy in terms of color scheme and consistency.

- **Contextual Fit:** Evaluates how well the image fits the broader context implied by the prompt, including aspects like mood, setting, and style.
- **Overall Appeal:** Provides a holistic assessment of the image’s attractiveness and visual impact, taking into account its general appeal to viewers.

### 10. FLORA Dataset

#### 10.1. Dataset Creation and Filtering Process

To create the FLORA dataset, we employed a multi-stage filtering and description process to ensure that the images met quality standards and contained only the desired fashion elements. Below, we describe the stages of filtering, noise removal, and detailed description generation, along with the prompts used at each step.

**Initial Filtering of Noise Using VLM Model:** In the initial filtering stage, we used a VLM model (LLaVa 32b) to identify and remove images that did not meet the criteria for inclusion in the dataset. Specifically, we aimed to retain images that contained a single outfit sketch without extraneous objects. To achieve this, we provided each image with the following prompts and used the model’s responses to segregate the data:

**Prompt 1:** “Is there a single outfit present in the image? Yes or No?”

**Prompt 2:** “Is the outfit present in the image a sketch? Yes or No?”

**Prompt 3:** “Does the image only contain the sketch without any other objects? Yes or No?”

**Prompt 4:** “Are there multiple outfits present in the image? Yes or No?”

If the VLLM model answered “Yes” to the questions indicating the desired characteristics (single outfit, sketch format, no additional objects, and no multiple outfits), the image proceeded to the next filtering stage. If the answer to any of these prompts was “No,” the image was discarded.

**Watermark Detection and Removal:** For images that passed the initial filtering, we implemented an additional check to detect and remove watermarks, which could interfere with model training. At this stage as well we utilized the LLaVa 32b with the following prompt:

**Prompt:** “Does this image contain a watermark? A watermark may appear as text or a logo superimposed over the image. Yes or No”

If the model identified a watermark (“Yes” response), we performed image inpainting to remove the watermark, as described in the main paper. This ensured that the images in the dataset were clean and free from visual obstructions.

**Input Prompt Generation:** Once the images were filtered, we used GPT-4o to generate precise and comprehensive descriptions of each outfit. This process involved a multi-turn approach, where each turn focused on describing a specific aspect of the image. The following prompts were used to extract detailed information:

**Model Pose Description:** “Describe the model’s posture. Is the model standing, sitting, walking, or in any other specific pose? Detail the position of the model’s hands, legs, and overall body stance. Provide enough detail so that someone reading the description could recreate the sketch with high accuracy. Note: Generate a response in a single paragraph with not more than 50 words. Please note that - while describing pose, do not describe the dress the model is wearing or do not use any adjectives. Just in simple words, explain the pose of the model, nothing else.”

**Outfit Description:** “Describe the outfit present in the image. Describe in a way that a fashion designer can read that description and create an exact similar sketch of the outfit. Use fashion design terminology. Describe garment type, fabric, cut, and any special features. Note: Generate a response in a single paragraph with not more than 200 words.”

**Color Details:** “Provide a detailed description of the color scheme used in the outfit. Mention the primary color, any secondary colors, and any unique color patterns. Note: Generate the response in a single paragraph with not more than 50 words. Just return color-related information.”

**Accessories Description:** “Mention and describe any accessories or additional design elements included in the sketch, such as belts, shoes, jewelry, or headpieces. Provide enough detail so that someone reading the description could recreate the sketch with high accuracy.

Note: Generate the response in a single paragraph with not more than 50 words. If no accessories are present, respond with ‘no additional accessories present’.”

This multi-turn approach allowed us to capture specific details of each image, resulting in a dataset that accurately reflects the visual and stylistic characteristics required for high-quality, fashion-focused AI training.

Additionally, we extracted information on the presence and gender of the model in each image using LLaVa 32b. By using this layered approach - initial filtering, watermark detection, and detailed multi-turn descriptions; we created a high-quality, fashion-specific dataset (FLORA) that supports the generation of accurate and stylistically rich images from textual descriptions. This structured dataset creation process ensures that the FLORA dataset is diverse, precise, and highly applicable to fashion-focused generative AI tasks.

## 10.2. Dataset Insights and Diversity Analysis

Figure 10 summarizes the gender representation and model presence in the FLORA dataset. Of the images, 97.5% (4,220) feature female outfits, 0.27% (12) male outfits, and 2.26% (98) show “no gender,” where the outfit is displayed without a model. Similarly, 97% of the images include a model wearing the outfit, while 3% display only the outfit. These distributions in the FLORA dataset are influenced by the types of fashion images commonly found on the internet. For example, the high percentage of female outfits and model presence results from the dataset being sourced from online data, where such trends are prevalent.

Our dataset consists of a wide array of fashion outfit styles, which we categorize into nine distinct classes, each with its own set of sub-classes. These terminologies include **Garment Types** comprising 29 sub-classes such as *blazers, gowns, hoodies, kimonos, skirts and jackets*. The **Styles & Details** class has 17 sub-classes including attributes like *sleeveless, bateau, turtle-neck and halter*. **Materials & Patterns** with 21 sub-classes describes fabric types and patterns like *silk, cotton, denim, satin, floral and striped*. **Construction & Detailing** includes 40 sub-classes covering elements such as *embroidery, beading, embellishments, metallic, cinched, knitting and vintage or retro aesthetics*. The **Technical & Functional** class has five sub-classes which focus on functional features such as *breathability, lightweight materials and detachable components*. **Occasion & Aesthetic** includes 18 sub-classes categorizing outfits by their intended use and style such as *casual, formal, traditional, sophisticated, beachwear and whimsical*. **Construction Techniques** with 10 sub-classes includes garment construction methods like *stitching, buttoning, zippers and lining*. **Detailing Techniques** with 19 sub-classes describes



Figure 9. Representation of a few classes from each of the 9 categories, showcasing a diverse range of design elements present in our FLORA dataset

specific design techniques like *applique*, *beading*, *draping*, *gathering*, *pleating* and *layering*. Finally, the **Finishing Techniques** class has five sub-classes that address finishing touches like *fading*, *top-stitching* and *softening*. The distribution of these terminologies across the dataset is presented in log-scaled figures (11 - 19), which provide an insightful representation of their relative prevalence.

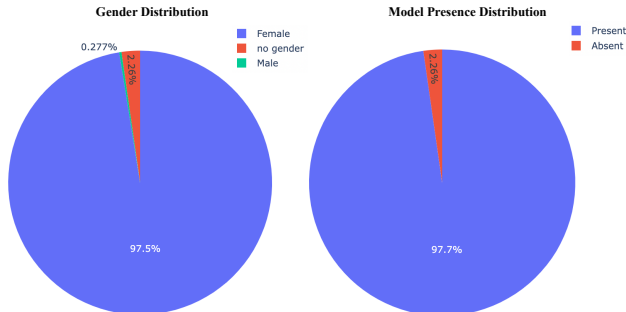


Figure 10. Distribution of gender representation and model presence in the FLORA dataset.

## 11. Ablation Study

In this section, we investigate the use of KAN adapters as an alternative to LoRA. Extending our previous ablation studies, we explore the effect of varying ranks for LoRA and downsample rates for KAN adapters. For this task, we choose FLUX as our baseline model for conducting the ex-

LoRA Rank		
LoRA Rank	FID↓	CLIP SIM↑
$r = 8$	8.76	0.2711
$r = 16$	8.13	0.2832
$r = 32$	7.92	0.2901
$r = 64$ (Default)	<b>7.88</b>	<b>0.2987</b>
KAN Downsample Rate		
Downsample Rate	FID↓	CLIPSIM↑
$m/16$	7.18	0.3298
$m/8$	6.66	0.3319
$m/4$	6.49	0.3401
$m/2$ (Default)	<b>6.05</b>	<b>0.3412</b>

Table 4. Ablation study comparing the effect of varying ranks for LoRA and downsample rates for KAN-adapters using FLUX as the baseline.

periments. Table 4 provides the CLIP-SIM and FID scores for different ranks and downsampling rates for the respective adapters.

**Effect of Rank on LoRA Performance:** For LoRA, we observe a progressive improvement in both CLIP-SIM and FID scores as the rank increases. The model achieves the highest performance at rank  $r = 64$ , yielding a CLIP-SIM of 0.2987 and an FID of 7.88. This indicates that increasing the rank allows LoRA to better capture domain-specific details relevant to our sketch generation task.

**Effect of Downsample Rate on KAN Performance:** The downsample rate in the KAN Adapter refers to the di-

dimensionality reduction applied to the input features. Specifically, as explained in section 4.3, the KAN adapter incorporates two main functions: the  $\phi_{down}$  and  $\phi_{up}$ .  $\phi_{down}$  projects the input features from the original dimensionality ( $m$ ) to a reduced dimensionality ( $n$ ), and the  $\phi_{up}$  projects the reduced-dimensional features back to their original size  $m$ . Here,  $n$  is the downsampling rate, which is hyperparameter and is decided by the ratio by which we want to reduce dimension (e.g.  $m/16$ ,  $m/8$ ,  $m/4$ ,  $m/2$ ). Where a smaller downsample rate ( $m/16$ ) implies greater reduction and larger rates ( $m/2$ ) retain more of the original feature space.

The ablation study, as shown in the table 4, evaluates the performance of KAN Adapters at different downsample rates. As the downsampling rate increases from  $m/16$  to  $m/2$  results in improvements in both CLIP-SIM and FID scores. This progression highlights the trade-off between dimensionality reduction and feature retention, with higher downsample rates striking an optimal balance between computational efficiency and model performance. These findings emphasize the importance of selecting an appropriate downsample rate to maximize the KAN Adapter’s effectiveness.

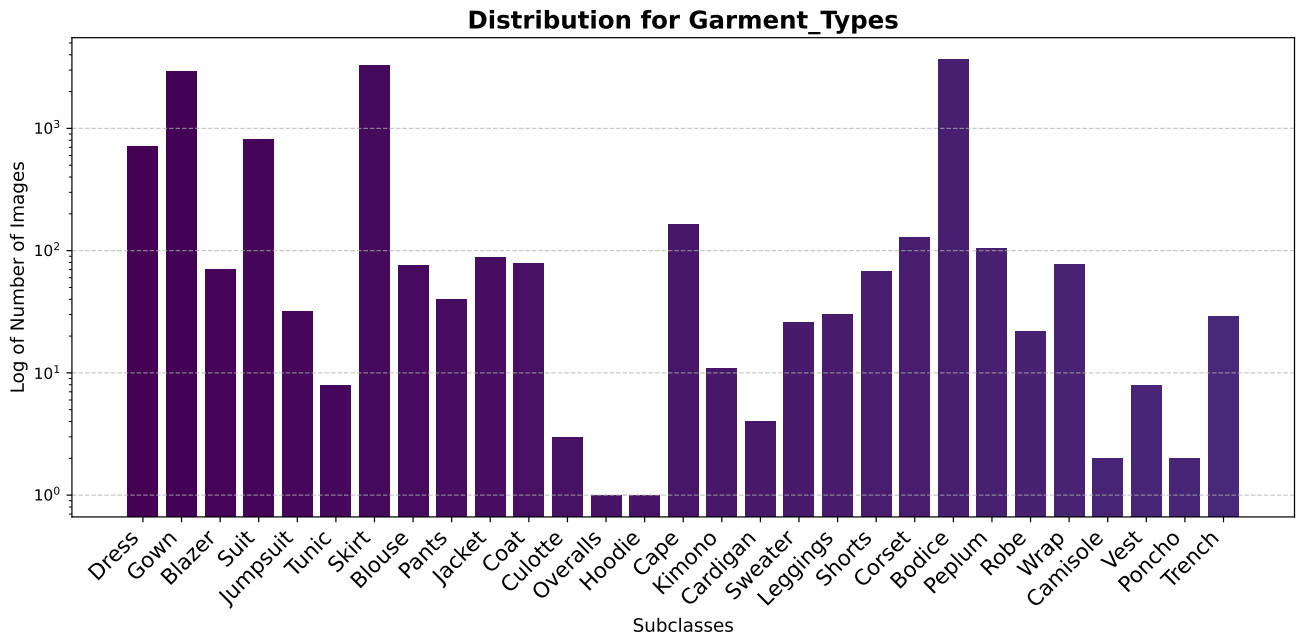


Figure 11. Image Distribution for 29 Garment Types available in FLORA

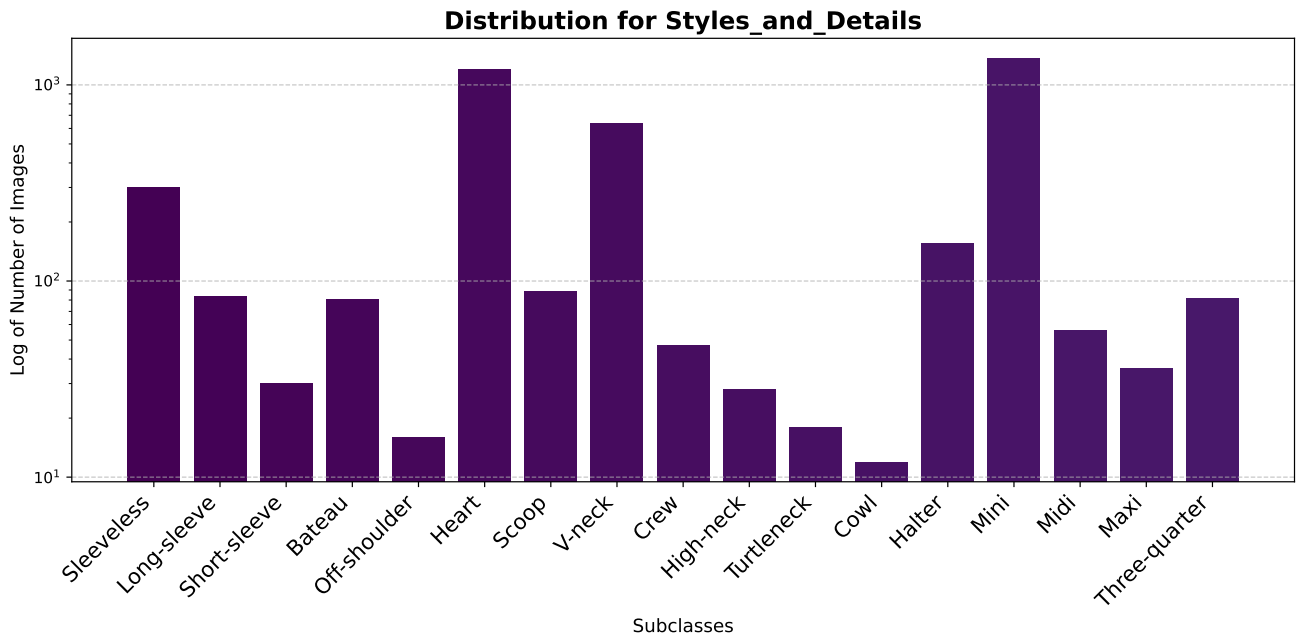


Figure 12. Image Distribution for 17 Styles

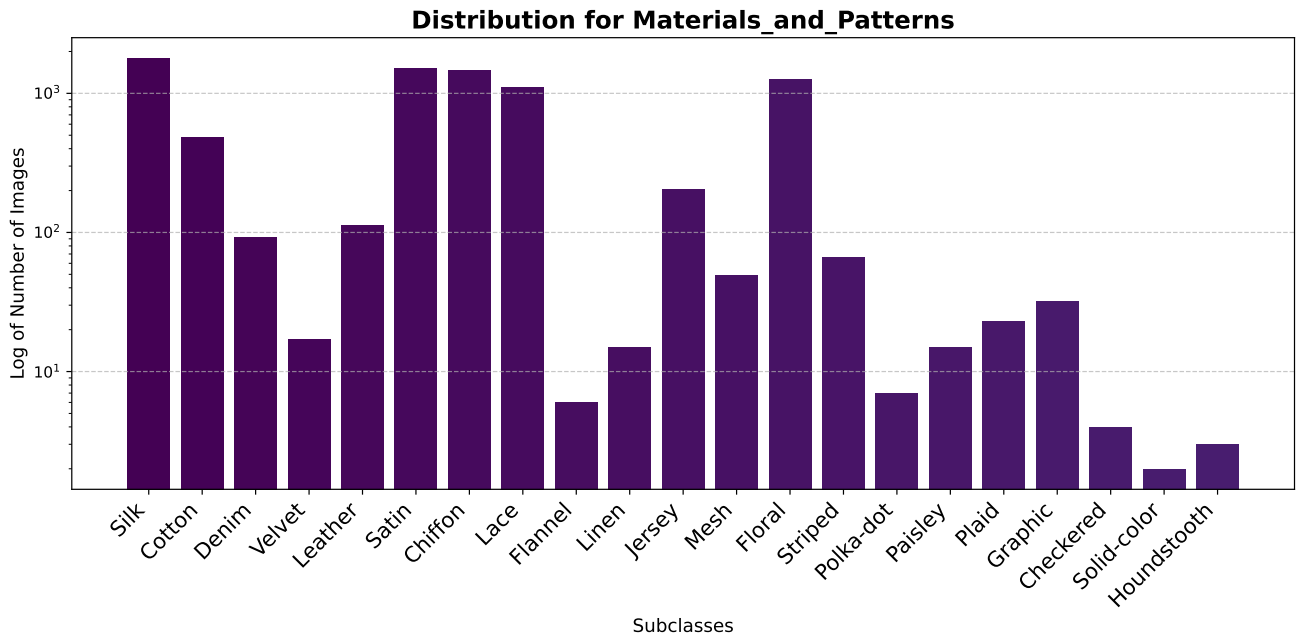


Figure 13. Image Distribution for 21 Materials & Patterns

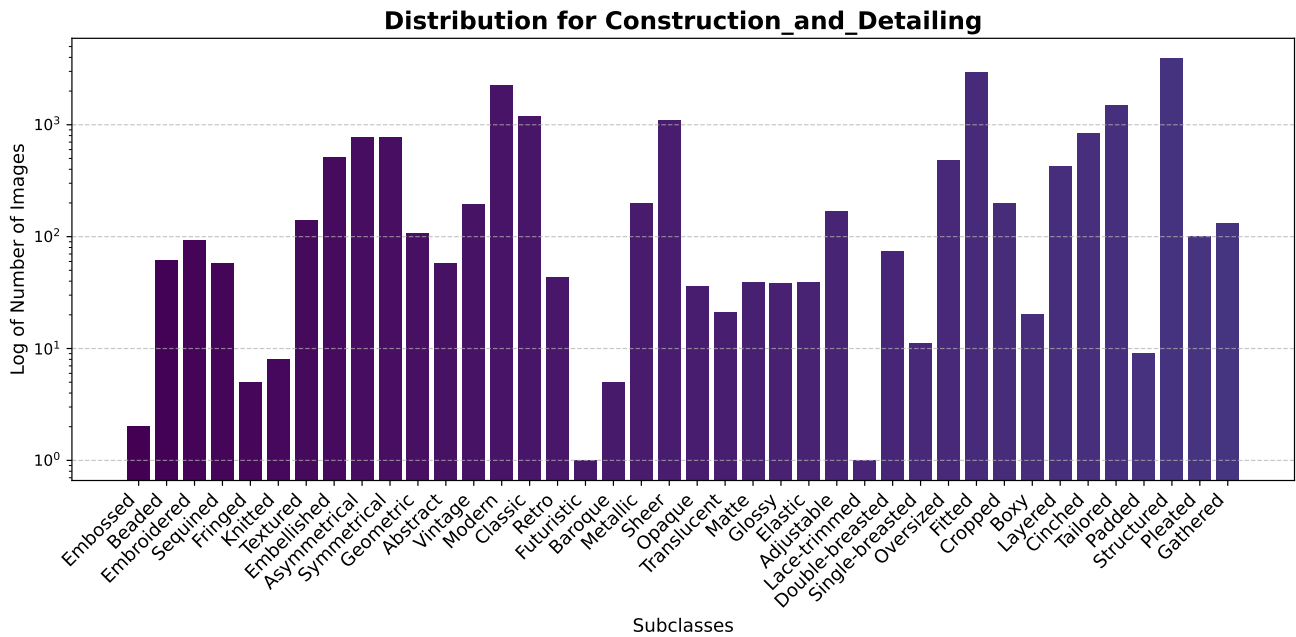


Figure 14. Image Distribution for 40 Construction styles



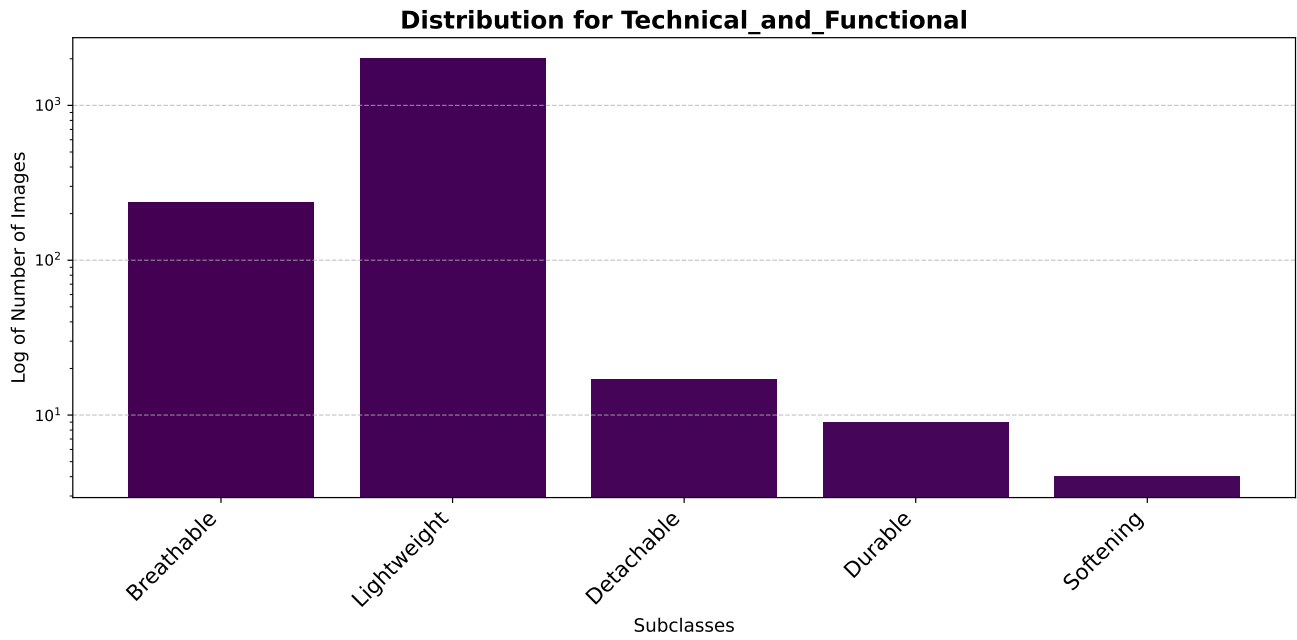


Figure 15. Image Distribution for Technical styles

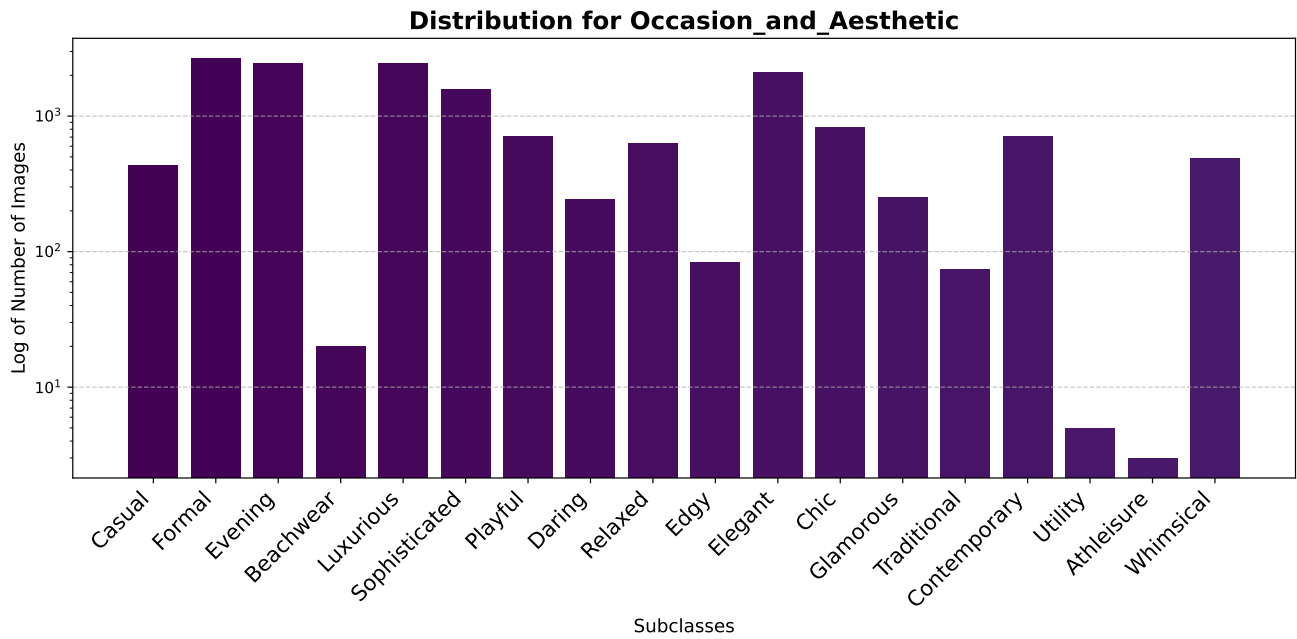


Figure 16. Image Distribution for 18 Occasion & Aesthetic styles

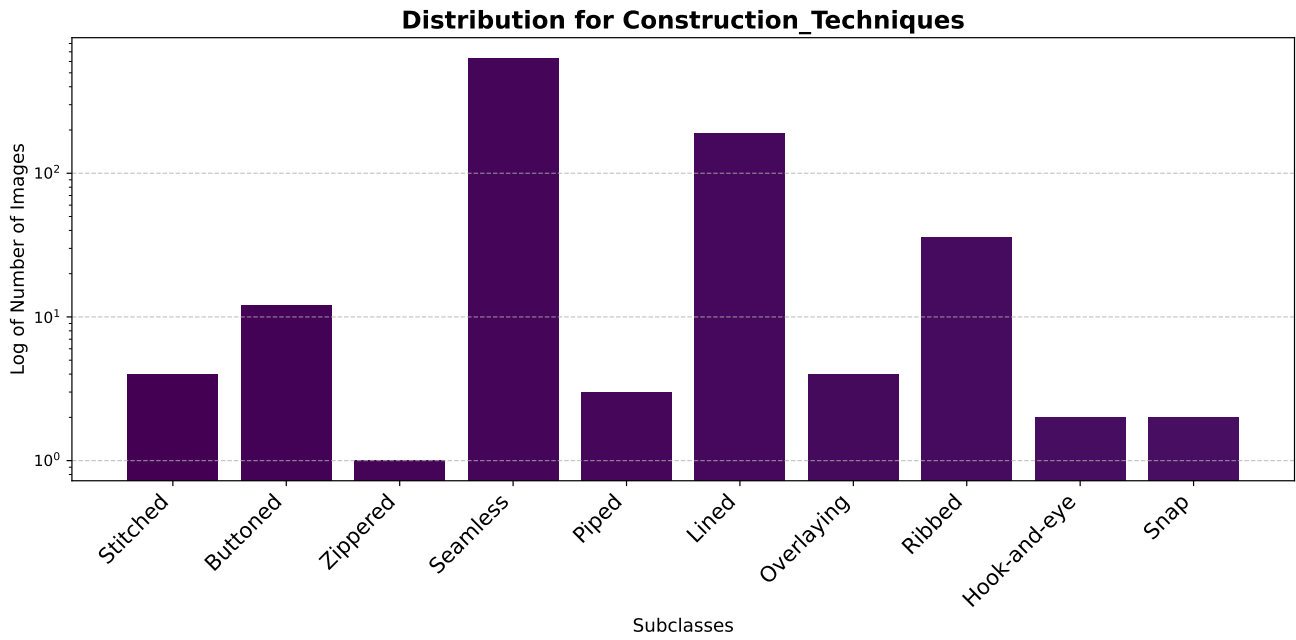


Figure 17. Image Distribution for 10 Construction techniques

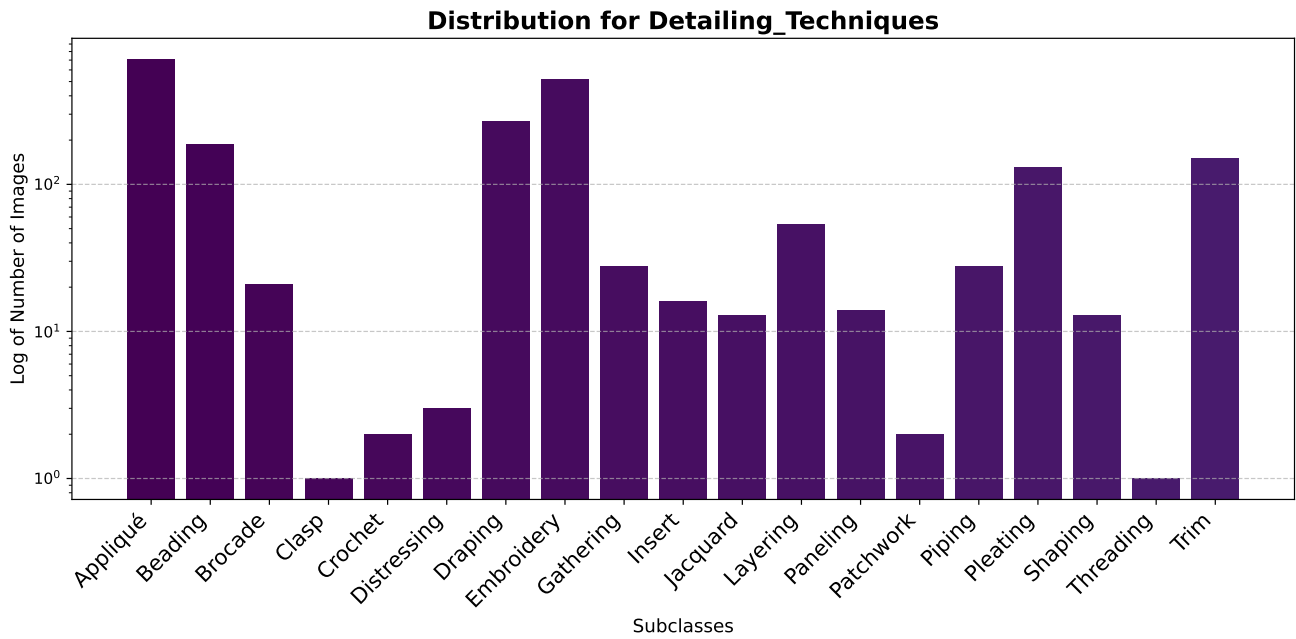


Figure 18. Image Distribution for 19 Detailing techniques

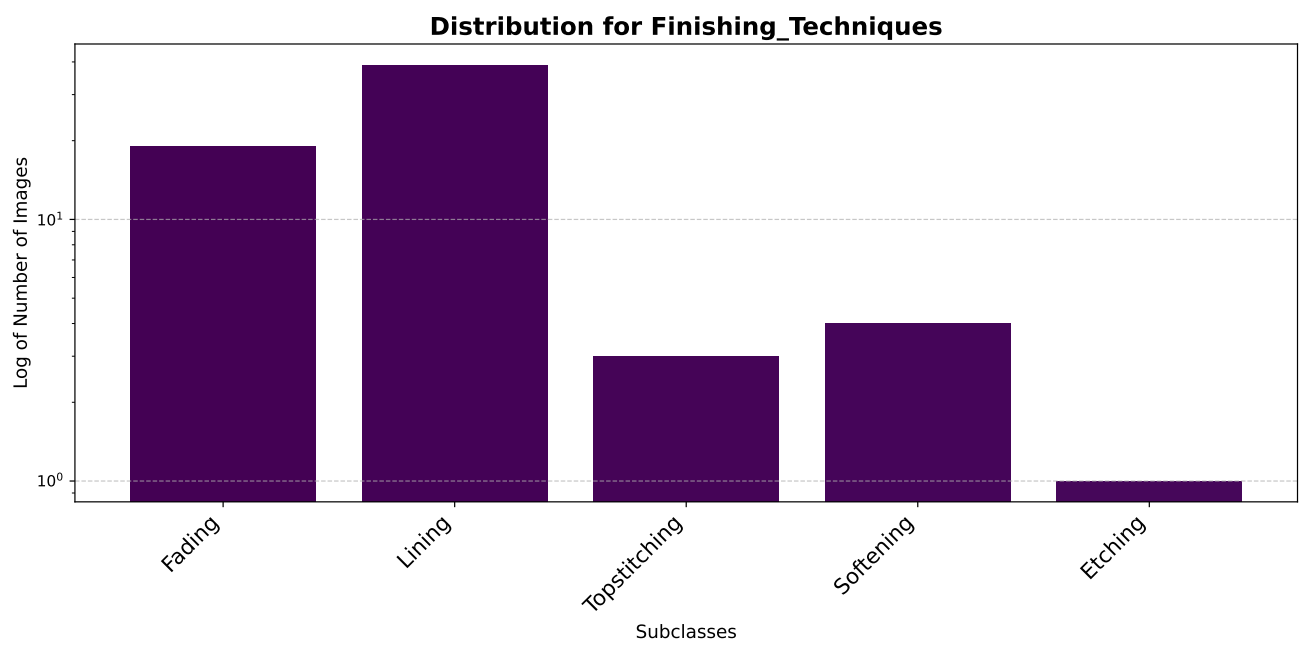


Figure 19. Image Distribution for Finishing techniques